

Chapter 2

Texture analysis by wavelet decomposition

In this chapter we go to review the main topics of this work. We start with a summary of the texture analysis methods, enumerating the different approaches taken over this theme and explaining several applications where texture has an important role. In a second part we explain in detail the tool that we have choose in order to analyze texture in this work. This wavelet decomposition explanations start with a fast historical review followed by some theoretical foundation of this theme and finally with some basic applications. In the last part of the chapter we try to merge these two worlds, and we analyze different solutions adopted in the literature.

2.1 Texture analysis

Texture is an important field in computer vision. Several applications were texture information plays a valuable role can be found among others in the medical imaging, scene analysis, remote sensing and quality control fields. Since the earliest works on texture analysis in 1970's the knowledge of this area has grown becoming nowadays one of the most active research fields in computer vision.

Texture is a term commonly used to describe properties of the surface of an object. One of the definitions we can find in Webster's dictionary is: "The characteristic physical structure given to a material, an object, etc., by the size, shape, arrangement, and proportions of its parts..." These properties are mainly related to a tactile sensation. When seeing texture images people uses similar attributes to the tactile perception to describe what is being perceived [99] although both perceptions can be not related.

If we consider how are these textures formed, we realize that they can be described in a variety of ways [104]. Texture can be generated from primitives or *textons* (texture elements) organized by placement rules or as a result of some stochastic process. We can found textures from purely deterministic, for example a brick wall, to purely random, as an image of sand.

2.1.1 Approaches to texture analysis

The main methodologies applied when analyzing texture are those related to structural, statistical, stochastic, and space-frequency models. Differences between these approaches lie on what is it assumed to be the underlying texture structure. For this reason the most suitable methodology for each application depends on the kind of texture:

- Structural methods consider texture from the point of view of formal languages theory. In this case, primitives forming repetitive patterns define images and these methods try to describe such patterns in terms of their construction rules. Structural approach is mostly carry out by document analysis community [92, 51].
- Statistical models characterize textures using joint probability distributions of image pixel intensities. Co-occurrence matrix [36] is the most popular and representative method of this group.
- Stochastic methods define image gray level as state variables and the texture has the probability of transition between those stages. Markov random fields [49] are probably the most widespread of this methodologies.
- Spatial-frequency models use the fact that most textures, due to their repetitive behavior, are easier to represent in the spectral domain than in the spatial one. Spatial-frequency approach to texture analysis have provide the most successful solutions to the problems of texture characterization. Their success is reflected in the large number publications in this field. Here we found techniques in which features are obtained studying new representations as spectral ones or conjoint representations of space and frequency. Fourier, Gabor, Wavelets are some of the most representative techniques of this group [78]. The approach we have used to study our images.

There are several books and articles that give overviews of the available methodology in the texture field [93, 79]. In these works the previous four categories are almost represented, maybe with different names.

2.1.2 Applications of texture analysis

There are a wide range of examples where texture recognition is and important part of the study of these problems. Some of the fields with several applications examples where texture has an important role are explained in the next paragraphs.

Machine Vision: There are several point in an industrial process where inspection of texture can be useful. Among them maybe quality control is the most outstanding. In most cases quality processes based on visual inspection are done manually, thus the possibility of automation by means of artificial vision is of great interest. Finish quality of an object or material is a visual impression defined by its texture; therefore texture analysis plays an important role in inspection. There are a lot of examples

of industrial inspection based on texture, for instance: classification of ceramic tiles to reduce over segmentation of the stock [57], description of wood texture in order to define criteria of aesthetic compatibility between boards [35].

Image retrieval: The amount of information that is accessible nowadays in its electronic version is very big compared to a few decades ago. Sometimes this information consists of images that contain in its turn new information that has not been annotated by hand. Searching over large databases of images is a laborious task more and more common. Therefore, any improvement on techniques related to this task is of great interest. Some contents in these repositories have texture as an important feature. Hence, applications including texture have been proposed [30, 71].

Medical imaging: Images on this field come from non-intrusive techniques as photography, x-ray, ultrasound, tomography, etc.; and from intrusive techniques as microscopic analysis of tissue. Texture is an important clue in several diagnoses that takes these images as part of the study. These examples come from early detection of mammographic lesions [34], cancer detection in liver cells [2], detection of distortion in trabecular bones [52], and classification of the pneumoconiosis disease degree [100].

Remote sensing: In this field images also come from different sensors. These sensors acquired different features of distant objects on which we want to perform some measurements. The use of spectral features for image classification is one of the standard techniques widely used in remote sensing, however, this classification is very limited if illumination conditions change. Texture features solve some of these problems [83] because they are invaluable clues for visual human inspection. Some applications in this field include terrain classification, cloud classification, urban/field classification, etc.

More information about other application fields as document segmentation [45], shape from texture [91], 1D texture, can be found in [77, 93].

Despite of the scope of the application, researchers use to face several common problems when they analyze texture information: classification, discrimination, description, identification, segmentation, and synthesis of textures. The work presented in this dissertation is mainly concerned about the classification, although, in one way or another, all these approaches are represented in this work. Segmentation of marble images can be associated to a classification and description problem; although it is in essence a segmentation problem it cannot be related to a typical texture segmentation problem. In the recognition of tiles we classify in order to discriminate samples. In the recognition of paints we classify in order to identify pigments. The final studies that try to characterize texture in a global way are concerned with classification and synthesis problems.

2.2 Wavelets

Nowadays, wavelets are one of the most important tools in the study of textures. If we do a fast review of the techniques used in segmentation, classification and synthesis of textures we will see that wavelets, including Gabor filters¹, become the most used tools in these kinds of works.

There are a number of introductory books on wavelets [1, 20, 63]. Among them it is fair to emphasize the Mallat's book [63] with a broad perspective on the principles of wavelets and the applications to 1D and 2D signal processing, besides being one of the most referenced authors in this field. We do in this section a short introduction to the wavelets because is the most important thread of all the following development we do in this work.

2.2.1 Introduction to wavelets

Wavelets come to light as a tool to study non-stationary problems. Such problems where Fourier analysis is not sufficient. At the beginning of 80's wavelets started as an alternative to the Fourier analysis in many fields as: mathematics, quantum physics, electricity, seismology, etc. The knowledge exchanged among these different fields some years ago gave rise to a bulk of new applications inside other fields. Specifically, a large number of problems were analyzed with this new tool in computer vision, specially image compression and texture analysis. However, almost every topic in computer vision has been studied with wavelets, as example: tracking [95], data fusion [47], database image retrieval [44], edge detection [64], layout segmentation [45], etc.

The basis of wavelets can be found in the beginning of twentieth century. The decomposition of a signal as a combination of several signals was developed in 1807 by Joseph Fourier. He devised a method to express a well-behaved function as an infinite sum of sinusoidal functions. In this way a function can be studied in terms of their spectral components. Wavelets perform a decomposition of a function as a sum of other functions, but unlike Fourier decomposition, these functions are local bases, have finite support, and are localized at different scales. It acts as if we have a window that can be positioned over any point of the function, moving the window we have a local analysis (localized) and varying the width of the window we can arrive to different detail levels (scale).

The field of image processing has taken this theory adapting it to their signals, basically extending the algorithms to 2D. But, it is not only a new transformation to work with. The features that images present, the statistics over the spatial domain make of wavelets an ideally tool for their analysis. Images, except restricted domains, have a non-stationary behavior. This non-stationary property force, in most cases, to perform a local study of this kind of signals. Measures we can take to characterize an image vary a lot over all their points due to this non-stationary behavior. For instance, images have contours, it means, discontinuities that breaks any possible

¹Gabor filters are considered as wavelets for most authors although they do not fit exactly in the definition. Nevertheless, they are seen as precursors of wavelets in the sense of non-orthogonal decomposition.

stationariness. Moreover, we found objects inside images with sizes and texture that also varies. Inside and image there are different scales where interest is greater. A frequency analysis of an image in some cases is sufficient, but in most cases we want more information, for example, where some features or patterns occur. With a frequency analysis we do not have a clear localization of where some patterns appear.

Still, wavelets do not substitute Fourier analysis in the image processing field, since they permit us to consider other approaches.

Wavelets are bounded functions with zero average. This implies that shapes of these functions are waves restricted in time. From this little wave (wavelet) comes their name. Their time-frequency limitation yields a good localization. Figure 2.1 shows two examples of wavelets widely used to illustrate this space-frequency localization concept. At the same figure we can see their Fourier transform spectrum that give us an idea of their frequency localization.

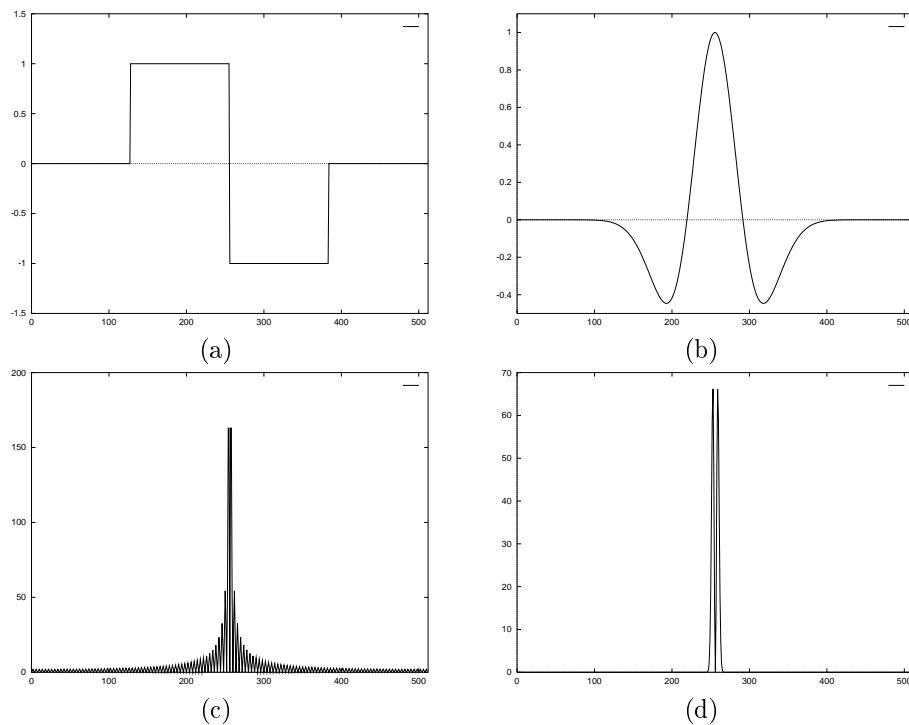


Figure 2.1: Functions used as wavelets: (a) Haar, (b) Mexican hat (Laplacian of Gaussian). And their Fourier transforms: (c), (d).

Starting from a function of the same type that functions showed before, $\psi(t)$, named mother wavelet, we are able to build a base, in the sense of a vector (function) base where we can decompose any vector (function). This base is generated by means

of translations and dilations of the mother wavelet,

$$\psi_{ab}(t) = \frac{1}{\sqrt{a}}\psi\left(\frac{t-b}{a}\right) .$$

To perform the study of a signal (function) with wavelet decomposition we obtain the coefficients of this signal in the previous generated base from this mother wavelet.

An important difference from the Fourier analysis is that functions of these bases are well-localized in space (or time) and scale (frequency) unlike functions used in Fourier analysis that are sine and cosine (complex exponential) that are well-localized in frequency but non-localized in space. Due to the fact of this localization, they permit the study of abrupt functions with a lower number of coefficients.

One of the first steps to solve the problem of the bad localization of the Fourier transform was proposed by Gabor in 1946. It consists on moving a fixed-duration window over the function and extracting the frequency content in that interval. This transformation has different names: STFT (Short Time Fourier Transform), Sliding Window Fourier Transform and, if the window is Gaussian, Gabor Transform. With this transform we have a better localization, we know what frequencies we have and where they are located over the signal. This transform is given by:

$$F(\Omega, \tau) = \int_{-\infty}^{\infty} f(t)g^*(t - \tau)e^{-j\Omega t} dt ,$$

where $g(t)$ is the window and $*$ represents the complex conjugate.

This transformation would be suitable for signals that are locally stationary, but globally non-stationary as speech signals. Image field usually associate the concept of Gabor filter to $g(t)e^{-j\Omega t}$, but for image is better to adapt the window width to the frequency content. Gabor propose Gaussian windows because is the function that reduces the uncertainty of the transformation to its minimum. It is related to the uncertainty principle of Heisenberg. According to it, the product of the uncertainties in time and frequency cannot be reduced below a certain constant. If we choose fixed windows the uncertainty boxes are equal in shape over the time-frequency space. If we choose an adapted window, although with the same area due to the uncertainty principle, boxes can be adapted to the contents.

Wavelets are function basis that share this outstanding property of being well localized spatially and in frequency. The name of wavelets comes form a short oscillating signal over a reduced interval (little wave). For all this things, wavelets are well adapted to represent short abrupt signals and also smooth functions.

2.2.2 Gabor wavelets

Gabor functions are an important family of filters used in computer vision because they can model some properties of the low level human visual system. They have been successfully used to explain the response of the visual cortex form the human visual system [21] and also in many applications as texture analysis and segmentation [12], motion analysis [38], face detection [27], etc. These filters can be explained in terms of wavelet transform and Short Fourier Transform.

There are some evidences that a part of the visual cortex acts as a directional and two-dimensional filter bank: in each position of the image a window is centered to select an area that is directional filtered (each filter with a preferred direction) and next is frequency filtered (band-pass filters). This double filtering process can be reduced to one, if we build a filter bank with preferred direction and spatial frequency band-pass in this direction as input parameters. Gabor filters are a family of filters fulfilling these requirements and also have a minimum of uncertainty over the spatial-frequency plane. Moreover, these filters can be adapted to the wavelets format, in the sense that can be expressed in terms of rotations, dilations and translations of a mother Gabor filter.

Several equivalent formulations of Gabor filters have been proposed. We start this introduction with the 1D case and we analyze the relation with the Short Time Fourier Transform (STFT). Later, we will explain the 2D expressions and finally, we show how should it be modified to become a Gabor wavelet decomposition.

The 1D impulse response to a Gabor filter is:

$$g(t) = e^{-t^2/2\sigma_t^2} e^{j2\pi\omega_0 t} = e^{-t^2/2\sigma_t^2} [\cos(2\pi\omega_0 t) + j \sin(2\pi\omega_0 t)] . \quad (2.1)$$

It is a Gaussian with σ_t variance, it is modulated by a complex exponential with ω_0 frequency. We perform the convolution of a signal with this Gabor filter in order to obtain the Gabor transformation at (ω_0, t) :

$$\begin{aligned} F(\omega_0, t) &= \int f(s)g(t-s)ds = \int f(s)e^{-(t-s)^2/2\sigma_t^2} e^{j2\pi\omega_0(t-s)} ds = \\ &= e^{j2\pi\omega_0 t} \int f(s)e^{-(t-s)^2/2\sigma_t^2} e^{-j2\pi\omega_0 s} ds , \end{aligned}$$

that, except for a phase change, is similar to the STFT with a Gaussian window. In practice most of the time this filtering is done in the frequency domain and not in the spatial domain. This is the Fourier transform of the filter:

$$G(\omega) = \int g(t)e^{-j2\pi\omega t} dt = \int e^{-t^2(2\sigma_t^2)} e^{-j2\pi(\omega-\omega_0)t} dt = \sigma\sqrt{2\pi} e^{-2\pi^2\sigma_t^2(\omega-\omega_0)} . \quad (2.2)$$

It is a real function, a Gaussian with variance equal to $\sigma_\omega = 1/2\pi\sigma_t$ and centered at ω_0 . $G(\omega)$ express the way as the filter modify each frequency component of the input signal around t . Therefore, parameters of a 1D Gabor filter are the frequency ω_0 and the extent around this frequency σ_ω .

2.2.3 Continuous and discrete wavelet transform

The continuous wavelet transform (CWT) [1], as the STFT, is a correspondence of $L^2(\mathbb{R}) \longrightarrow L^2(\mathbb{R}^2)$, but with a higher space-frequency localization. $L^2(\mathbb{R})$ and $L^2(\mathbb{R}^2)$ are, respectively, the space of real 1D and 2D functions with real variable and square integrable:

$$f \in L^2(\mathbb{R}) \iff \int_{-\infty}^{+\infty} |f(t)|^2 dt < \infty .$$

The CWT assign to each one of these functions a new function $W(a, b)$, but with two variables, which is defined from dilations and translations of a *mother* wavelet function:

$$\psi_{a,b}(t) = \frac{1}{\sqrt{a}} \psi\left(\frac{t-b}{a}\right) \quad (2.3)$$

$$W(a, b) = \int_{-\infty}^{\infty} \psi_{a,b}(t) f(t) dt = \langle \psi_{a,b}(t), f(t) \rangle . \quad (2.4)$$

It can be proved that CWT is invertible if the chosen wavelet $\psi(t)$ fulfill the *admissibility condition*:

$$C_\psi = \int_0^{\infty} \frac{|\Psi(\omega)|^2}{\omega} d\omega < \infty . \quad (2.5)$$

Then, the inverse transform is:

$$f(t) = \frac{1}{C_\psi} \int_{-\infty}^{\infty} \int_0^{\infty} \frac{1}{a^2} W(a, b) \psi_{a,b}(t) da db . \quad (2.6)$$

This equation can be see firstly as a way to reconstruct f once the CWT is known, and secondly how to express f as sum of wavelets $\psi_{a,b}$. We can say that f is a lineal combination of wavelets, for different values of a, b , each one weighted by a factor $W(a, b)$, as a vector can be expressed as a weighted sum of other vectors of a base.

The election of the wavelet ψ in the CWT, or later in the discrete transform, is only restricted to the admissibility condition of Eq. (2.5). In this equation, $\Psi(\omega)$ is the Fourier transform of $\psi(t)$. If $C_\psi < \infty$ we need that $\Psi(0) = 0$. Therefore, as the Fourier transform of a signal at $\omega = 0$ is its average, $\int_{-\infty}^{\infty} \psi(t) dt = 0$. A way to get it is that $\psi(t)$ oscillate around the x axis, having positive and negative values that finally sum to zero. Besides, for practical reasons, ψ is chosen concentrated in both axis: space and frequency. Therefore, $|\psi(t)|$ should decrease when $|t|$ increase (good spatial localization). Choosing accurately the oscillation shape we can obtain good frequency localization.

The CWT has two drawbacks: redundancy and impossibility to calculate it in practice. It is redundant because we are representing a real function $f(t)$ with another function with two variables $W(a, b)$ (from 1D to 2D). It is impossible to implement it computationally because their parameters a, b are continuous. We try to solve these two problems discretizing (sampling) the parameters. One way to discretize the dilation parameter is $a = a_0^m$, $m \in \mathbb{Z}$, $a_0 \neq 1$ constant. Thus, we get a series of wavelets ψ_m , of width, a_0^m . Usually we take $a_0 > 1$, although it is not important because m can be positive and negative. Often a value of $a_0 = 2$ is taken. For $m = 0$ we make b to be only integer multiples (positives and negatives) of a new constant b_0 . This constant is chosen in such a way that translations of the mother wavelet, $\psi(t - nb_0)$, be so close as to cover the whole real line. Then, the election of $b = nb_0 a_0^m$ assures that wavelets at m level,

$$\psi_{m,n}(t) = a_0^{-m/2} \psi\left(\frac{t - nb_0 a_0^m}{a_0^m}\right) = a_0^{-m/2} \psi(a_0^{-m} t - nb_0) , \quad (2.7)$$

cover the entire real axis as also do the translations $\psi(t - nb_0)$. Summarizing, the discrete wavelet transform (DWT) consists of the two following discretizations in Eq. (2.4),

$$a = a_0^m, \quad b = nb_0 a_0^m, \quad m, n \in \mathbb{Z}, \quad a_0 > 1, b_0 > 0 . \quad (2.8)$$

Then, we must answer to these questions:

- Can we express every function $f(t) \in L^2(\mathbb{R})$ as a contribution (weighted sum) of this set of discrete wavelets? That is, the following equations can be written for some f, ψ ?

$$f(t) = \sum_{m=-\infty}^{\infty} \sum_{n=-\infty}^{\infty} d_{m,n} \psi_{m,n}(t) \quad (2.9)$$

$$d_{m,n} = \langle f(t), \psi_{m,n}(t) \rangle . \quad (2.10)$$

In other words, does the linear combination of wavelets $\{\psi_{m,n}(t)\}_{m,n \in \mathbb{Z}}$ spans the function space $L^2(\mathbb{R})$? If it does right, we say that these base functions are complete.

- If it is complete, it means that it is redundant? That is, can we manage without one or more functions $\psi_{m,n}$ and still have a complete set? In this later case, the set $\{\psi_{m,n}(t)\}_{m,n \in \mathbb{Z}}$ is not linear independent.
- If it is complete, which is the longest discretization step (coarsest) that we can afford, in order to achieve a non-redundant set?

The answer to these questions leads us to the multiresolution analysis of the next section. But before processing, we are going to briefly introduce the concept of *frame*. A frame is a complete set of functions that, though it is able to span $L^2(\mathbb{R})$, it is not a base because lacks the property of linear independence. Wavelets frames

- Do not satisfy Parseval's theorem:

$$\|f\|^2 = \langle f(t), f(t) \rangle = \int |f(t)|^2 dt ,$$

but there are two constants $0 < A < B < \infty$ such that,

$$A\|f\|^2 \leq \sum_m \sum_n |d_{m,n}|^2 \leq B\|f\|^2 . \quad (2.11)$$

- The expansion of a function is not unique, that is, there are several wavelet decompositions that can generate one same function f .

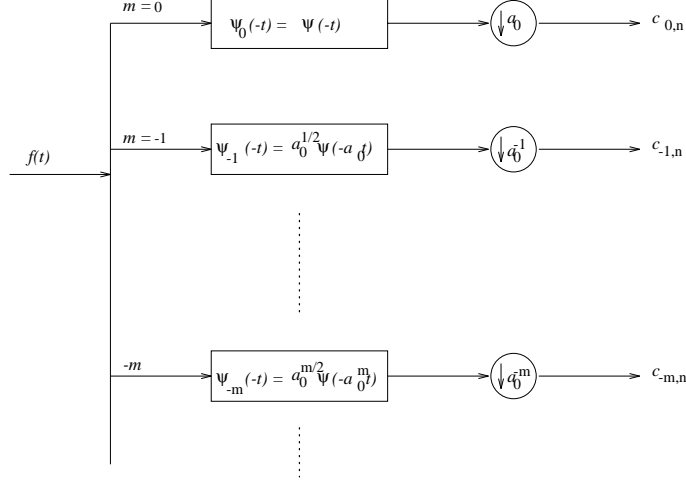


Figure 2.2: Discrete wavelet transform as a bank of filters. “ $\downarrow a_0$ ” denotes to take one out of a_0 samples (downsampling).

A frame is named *tight* when $A = B = 1$. But even this not guarantees the linear independence and therefore having redundancy. A frame is named *exact* when removing one of the functions leaves incomplete the set of functions. Finally, a tight and exact frame establish an orthonormal base of $L^2(\mathbb{R})$. Therefore,

$$\langle \psi_{m,n}(t), \psi_{m',n'}(t) \rangle = \int \psi_{m,n}(t) \psi_{m',n'}(t) dt = \delta_{m-m', n-n'} , \quad (2.12)$$

that is, they are orthonormal for the two indices. This means that at a same scale m they are orthonormal in the space and also among scales. The multiresolution analysis tries to build orthonormal bases for a dyadic grid, where $a_0 = 2, b_0 = 1$, which besides have a compact support region.

Finally, we can imagine the coefficients $d_{m,n}$ of the DWT as the sampling of the convolution of signal $f(t)$ with different filters $\psi_m(-t)$, where $\psi_m(t) = a_0^{-m/2} \psi(a^{-m} t)$ (see Fig. 2.2):

$$\begin{aligned} y_m(t) &= \int f(s) \psi_m(s-t) ds \\ d_{m,n} &= y_m(na_0^m) . \end{aligned}$$

As the frequency increases and the spatial width decreases, thus being closer the translations of the dilated mother wavelet, unlike Fourier transform where translations of analysis are at the same distance for all the frequencies (see Fig. 2.3).

2.2.4 Multiresolution analysis

The multiresolution analysis (MRA) proposed in [62] is another representation in which the signal is a sum of one approximation at a certain level L with L detail

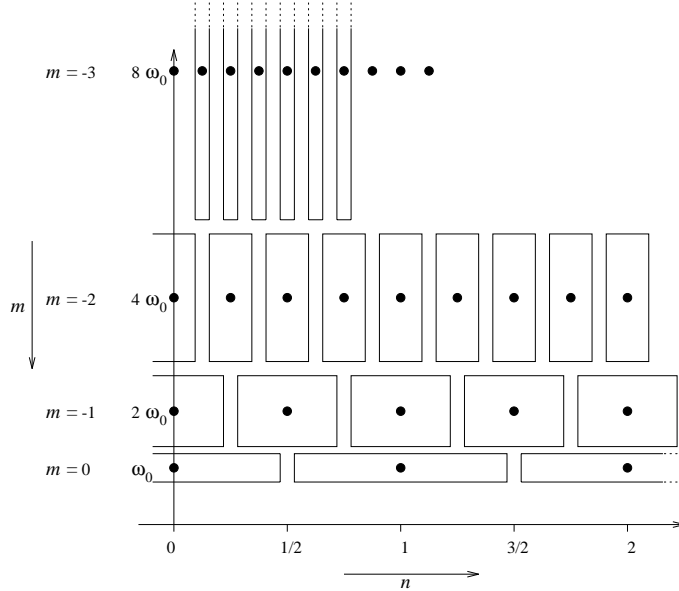


Figure 2.3: Diadic grid ($a_0 = 2, b_0 = 1$)

terms at different (higher) resolutions. This transform is also known as the fast wavelet transform. The representation is an orthonormal decomposition instead of a redundant frame and therefore the number of samples that defines a signal is the same that the number of coefficients of their transform. A fact that should be emphasized is that several techniques, already known as subband codification o pyramids, can be interpreted in terms of the MRA. Besides, MRA has been used successfully in a big amount of applications: image compression, filtering, image analysis, texture classification, image database indexing, etc.

Formulation

A multiresolution analysis consists on a sequence of function subspaces of successive approximation. They are spaces of functions of $L^2(\mathbb{R})$, that fulfill the next properties:

1. Nesting

$$\dots \subset V_2 \subset V_1 \subset V_0 \subset V_{-1} \subset V_{-2} \subset \dots \tag{2.13}$$

2. Completeness

$$\bigcap_{m \in \mathbb{Z}} V_m = \{0\} \ , \quad \bigcup_{m \in \mathbb{Z}} V_m = L^2(\mathbb{R}) \ . \tag{2.14}$$

If we named P_j the projection operator of a function over the V_j space, then this condition say that the approximations of a function tend to this function: $\lim_{j \rightarrow \infty} P_j f = f$ for all $f \in L^2(\mathbb{R})$. There are a lot of spaces that fulfill Eq. (2.13) and (2.14) but without relation to the multiresolution topic. This is a consequence of an additional condition:

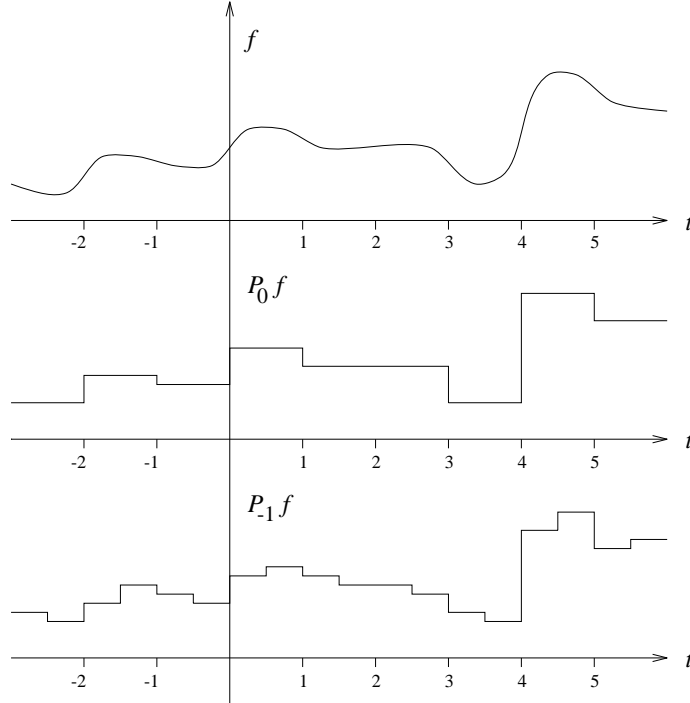


Figure 2.4: Function f and its projections in the V_0 and V_{-1} spaces

3. Multiresolution

$$f(t) \in V_j \iff f(2^j t) \in V_0, \quad \text{or} \quad f(t) \in V_j \iff f(2t) \in V_{j-1}. \quad (2.15)$$

This means that all the V_j spaces are scaled versions of a central space V_0 . The simplest example of spaces fulfilling this requirement (Eq. (2.13)–(2.15)) is the MRA of Haar. In it, V_j is the space of functions of $L^2(\mathbb{R})$ that are constant on the intervals $[2^j k, 2^j(k+1))$ for some fixed integer k (Fig. 2.4). This example also fulfills a new condition of the MRA:

4. Invariance to integer translations of V_0

$$f(t) \in V_0 \implies f(t-n) \in V_0, \quad \forall n \in \mathbb{Z}. \quad (2.16)$$

Therefore, translations by a multiple of 2^j of a function of the space V_j also belongs to V_j :

$$f(t) \in V_j \implies f(t-n2^j) \in V_j, \quad \forall n \in \mathbb{Z}. \quad (2.17)$$

Hence, the translation step to obtain this invariance depends on the scale j . For instance, at V_0 the step is 1, $1/2$ at V_{-1} , and $1/4$ at V_{-2} , etc.

5. Base property.

There is a function $\phi \in V_0$, named scaling function, in such a way that the set of its integer translations $\{\phi(t - n); n \in \mathbb{Z}\}$ is an orthonormal base of V_0 , that is,

$$\langle \phi(t - n), \phi(t - n') \rangle = \delta(n - n') \quad \forall n, n' \in \mathbb{Z} , \quad (2.18)$$

$$\text{span}\{\phi(t - n); n \in \mathbb{Z}\} = V_0 . \quad (2.19)$$

The first equation expresses orthonormality. In the second one, *span* denotes the space generated by a set of functions, that is, integer translations of ϕ form a frame of V_0 .

Now, we define a new function²:

$$\phi_{j,n}(t) = 2^{-j/2} \phi(2^{-j}t - n), \quad j, n \in \mathbb{Z} . \quad (2.20)$$

It is a dilated (by 2^{-j}), translated and scaled (by $2^{-j/2}$) version³ of $\phi(t)$. Then, $\{\phi_{j,n}; n \in \mathbb{Z}\}$ is a orthonormal base of V_j , and this means that

$$\langle \phi_{m,n}, \phi_{m,n'} \rangle = \delta(n - n') \quad \forall n, n' \in \mathbb{Z} , \quad (2.21)$$

$$\text{span}\{\phi_{m,n}; n \in \mathbb{Z}\} = V_m, \quad m \in \mathbb{Z} . \quad (2.22)$$

We define the P_j operator as the orthonormal projection of functions of L^2 over the space V_j . Projection of a function f over V_j is a new function that can be expressed as a linear combination (weighted sum) of the functions that form the orthonormal base of V_j . Coefficients of the combination of each base function is the scalar product of f with the base functions, i.e. the projection of f over the base functions:

$$P_j f = \sum_{n \in \mathbb{Z}} \langle f, \phi_{j,n} \rangle \phi_{j,n} , \quad (2.23)$$

where scalar product between functions of L^2 is a measure of their overlapping.

$$\langle f, g \rangle = \int_{-\infty}^{\infty} f(t)g(t)dt . \quad (2.24)$$

Before, we have pointed out the nesting condition of the V_j spaces, $V_j \subset V_{j-1}$. Well, now we require that if $f \in V_{j-1}$ then or $f \in V_j$ or f is orthonormal to all the V_j

²In some works $\phi_{j,n}(t) = 2^{j/2} \phi(2^j t - n)$. Then, as j increases the function is faster and the nesting property notation is reversed: $\dots \subset V_{-2} \subset V_{-1} \subset V_0 \subset V_1 \dots$

³The scaling condition can be expressed also as $f(t) \in V_0 \implies f(2^{-j}t) \in V_j$. Therefore, if $\{\phi_{0,n}; n \in \mathbb{Z}\}$ is a base of V_0 , $\{\phi_{j,n}; n \in \mathbb{Z}\}$ it will be also of V_j because V_j is precisely the space of the functions of V_0 dilated in this way. The scaling constant $2^{-j/2}$ attain norm equal to 1 if $\phi_{0,n}$ also has norm 1.

functions, that is, we divide V_{j-1} in two disjoint parts: V_j and other space W_j , such that if $f \in V_j, g \in W_j, f \perp g$ or equivalently, $\langle f, g \rangle = 0$ or even $V_j \perp W_j$. Then, we say that W_j is the orthonormal complement of V_j in V_{j-1} :

$$V_{j-1} = V_j \oplus W_j . \quad (2.25)$$

Symbol \oplus is the direct sum, the addition of orthonormal spaces. Applying Eq. (2.25) recursively and taking into account the completeness condition Eq. (2.14) we see that

$$\dots \oplus W_{j-2} \oplus W_{j-1} \oplus W_j \oplus W_{j+1} \oplus \dots = \bigoplus_{j \in \mathbb{Z}} W_j = L^2 . \quad (2.26)$$

Hence, we can write that

$$P_{j-1}f = P_j f + \sum_{n \in \mathbb{Z}} \langle f, \psi_{j,n} \rangle \psi_{j,n} . \quad (2.27)$$

This equation tells us an important thing that gives sense and usefulness to this wavelet decomposition. First, we said that projecting a signal f in a space V_j gives us a new signal $P_j f$ that is an approximation of the initial signal. Secondly, we have a hierarchy of spaces “ $\dots V_{j+1} \subset V_j \subset V_{j-1} \subset \dots$ ”. Therefore, $P_{j-1}f$ will be a better approximation (more reliable) than $P_j f$. How can we go from an approximation to the next better approximation? The expression of Eq. (2.27) tell us: we must add the projection of the signal over W_j . Hence, if V_j are approximation spaces, then W_j are *detail spaces*. The less j , the finer the details represented by W_j are.

Notice another feature of the MRA that makes interesting in practice the previous remark. Applying Eq. (2.25) repeatedly,

$$\begin{aligned} V_j &= V_{j+1} \oplus W_{j+1} = V_{j+2} \oplus W_{j+2} \oplus W_{j+1} = \dots \\ &= V_L \oplus W_L \oplus W_{L-1} \oplus \dots \oplus W_{j+1} . \end{aligned} \quad (2.28)$$

Graphically we have a tree of spaces in which edges (branches) represent the relation of inclusion (Fig. 2.5). We define a new projection operator, not in the approximation spaces V_j but in the W_j details:

$$Q_j f = \sum_{n \in \mathbb{Z}} \langle f, \psi_{j,n} \rangle \psi_{j,n} . \quad (2.29)$$

Then, by Eq. (2.28), we can express f as a sum of one approximation at a certain scale L (higher L means lower scale and poor approximation without detail) plus L functions of detail at higher scales. Each detail function is the loss due to passing from an approximation at scale j to the next $j + 1$,

$$P_j f = P_{j+1} f + Q_{j+1} f = \dots = P_L f + \sum_{k=j+1}^L Q_k f . \quad (2.30)$$

Finally, a property we need to build ψ wavelet from ϕ . We notice that a consequence of Eq. (2.25) and (2.13) and also that $W_j \perp W_k$ if $j \neq k$, that is, functions $\psi_{j,n}$ are orthonormal function intra-scale and also inter-scale:

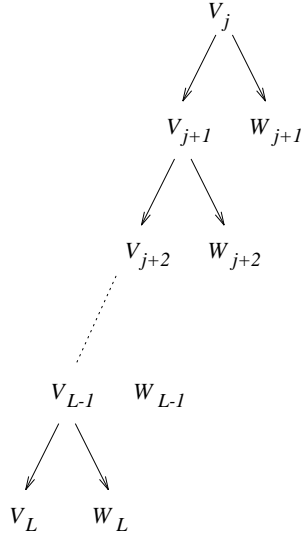


Figure 2.5: Tree of approximations and details

$$\langle \psi_{m,n}, \psi_{m',n'} \rangle = \delta(m - m', n - n') . \tag{2.31}$$

Construction of ψ from ϕ

From the previous five conditions of the MRA and the properties of ϕ and ψ , we can deduce two useful equations in order to apply MRA to discrete signals and to build ψ .

- Dilation equation.

$\phi \in V_0$ and $V_0 \subset V_{-1}$. V_{-1} has as an orthonormal base $\{\phi_{-1,n}; n \in \mathbb{Z}\}$. Therefore, we can express ϕ as a linear combination of these functions,

$$\phi = \sum_n h_n \phi_{-1,n} \text{ with } h_n = \langle \phi, \phi_{-1,n} \rangle ,$$

since $\phi_{-1,n}(t) = \sqrt{2}\phi(2t - n)$,

$$\boxed{\phi(t) = \sqrt{2} \sum_n h_n \phi(2t - n)} \tag{2.32}$$

- Basic wavelet equation

$\psi \in W_0$ and $W_0 \subset V_{-1}$ because $V_{-1} = V_0 \oplus W_0$. Equal than before, we can express it as a linear combination of functions of the base V_{-1} :

$$\psi = \sum_n g_n \phi_{-1,n} \text{ with } g_n = \langle \psi, \phi_{-1,n} \rangle ,$$

$$\boxed{\psi(t) = \sqrt{2} \sum_n g_n \phi(2t - n)} \quad (2.33)$$

2.2.5 À trous algorithm

The *à trous* algorithm is a redundant and stationary transform. It means that the volume of data increases with this transform and decomposition coefficients do not depend on their position. The redundancy is not good if our goal is to compress data, which is not our case. And stationariness is a desirable property for signal analysis, just what we want to do now. This property of stationariness, also known as translation invariance, arises because the decimation step is not performed. The filtering process consists of performing a convolution of the samples with a kernel, but in this case the distance between samples involved in the convolution increases in a factor 2 from one scale to the next. In the previous MRA, scheme we performed at this point a decimation step, but in the *à trous* algorithm we must to enlarge the convolution kernel adding zeros between their coefficients. A metaphor of this operation is to perform a transform ‘with holes’. This idea is used for naming the algorithm keeping its French root, *algorithme à trous*.

In the MRA we can see the initial discrete signal $c_0(k)$ to be analyzed as a projection of continuous function $f(x)$ on V_0 ,

$$c_0(k) = \langle f(x), \phi(x - k) \rangle = \int_{-\infty}^{\infty} f(x) \phi(x - k) dx . \quad (2.34)$$

The projection on a subspace V_i ,

$$c_i(k) = \langle f(x), \frac{1}{2^i} \phi\left(\frac{x}{2^i} - k\right) \rangle , \quad (2.35)$$

is then an approximation of c_0 at scale or resolution i .

Conversely, in the *à trous* transformation we do not perform the decimation step. Then, the approximation coefficients are now:

$$c_i(k) = \langle f(x), \frac{1}{2^i} \phi\left(\frac{x - k}{2^i}\right) \rangle . \quad (2.36)$$

However, we need some expression which allows the calculation of detail and approximation coefficients of a scale i from those of the previous scale. This is because we do not know the continuous function $f(x)$ but its discrete approximation c_0 . In the *à trous* algorithm, despite of the non-orthogonality of the subspaces V_i and W_i , we still have a sequence of embedded subspaces. As the translations of $\phi(x)$ span V_0 and $\phi(x/2) \in V_1 \subset V_0$,

$$\frac{1}{2} \phi\left(\frac{x}{2}\right) = \sum_n h(n) \phi(x - n) , \quad (2.37)$$

where $h(n)$ is a kernel filter associated with the scaling function $\phi(x)$. Then, from (2.36) and (2.37), we see that the approximation coefficients at scale $i+1$ are calculated by means of the discrete convolution of coefficients at scale i with a filter h ,

$$c_{i+1}(k) = \sum_n h(n) c_i(k + n2^i) . \quad (2.38)$$

The wavelet or detail coefficients w_i are computed as the difference between two consecutive scales,

$$w_i(k) = c_i(k) - c_{i-1}(k) ,$$

The reconstruction step of this algorithm is simply the sum of all the coefficients and the coarsest approximation:

$$c_0(k) = c_N(k) + \sum_{i=1}^N w_i(k) . \quad (2.39)$$

2.2.6 Wavelet packets

Wavelets are a good analysis tool for many image-based applications, but in some cases the frequency content of these images is not centered at the origin. For signals with a distribution of their information at middle or high frequencies it would be useful to have a similar tool where the analysis could be focused [106].

Wavelet decomposition can be seen as a particular case of a more general transformation, the wavelet packets transform. Wavelet packets are built as linear combinations of wavelets. They also form a base with some of the properties of wavelets such as orthogonality, smoothness and localization.

Coefficients of the discrete wavelet packet transform are calculated in a recursive way similar to the procedure followed in Sec. 2.2.4. When we perform a 1D decomposition (*DWPA*: discrete wavelet packet analysis) at each step of the transformation for we must open a binary tree. On one hand, one of the branches of the analysis tree decompose the approximation term filtering it with a low pass and a high pass filters to get the respective approximation and detail coefficients at the next level. This previous process it exactly the same used in the MRA and the spaces related to this partial decomposition form also a tree structure as we can see at Fig. 2.5. On the other hand, in the other branch we also perform the same process but to the details. Thus at each step of the decomposition, for each node two new set of coefficients are calculated. The tree structure of this transform can be see in Fig. 2.6 where a signal with coefficient x_i is decomposed in a tree.

The tree built at the analysis stage has a lot of redundant information, but this complete tree expansion is not necessary at all. The reconstruction stage (*DWPS*: discrete wavelet packet synthesis) is done from a subset of nodes of the tree. For these nodes we apply the same reconstruction as in the wavelet case. From an approximation node and the corresponding detail node we can obtain the preceding node (approximation or detail). The nodes that must be selected to obtain a perfect reconstruction can be chosen in several ways, but it must be complete, that is, you must have the necessary and sufficient information (nodes) to reconstruct any predecessor.

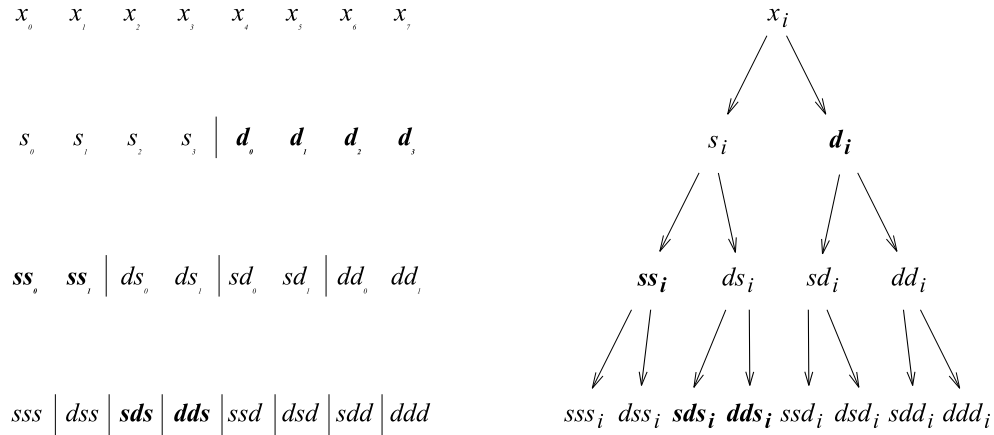


Figure 2.6: Decomposition in *wavelet packets* ($N = 8, L = 3$). Bold-faced coefficients are one of the possible elections to reconstruct completely the signal.

Figure 2.6 shows a discrete wavelet packet analysis tree. For the sake of explanation let's consider a dyadic decomposition. We start from a signal of length N (eight coefficients in the example) and we filter this signal with H and G filters whose coefficients define a wavelet and a scaling function as in the MRA case (see Eq. (2.32) and (2.33)). This process is performed as many times as levels we want in the decomposition. Let be L the number of levels ($L \leq \log_2 N$). Once we obtain the analysis tree, we can reconstruct by choosing a subset of appropriate nodes. For example: all the pure detail nodes and the last approximation as in a wavelet reconstruction, or all the nodes at a certain level, or all the bold-faced nodes in Fig. 2.6.

Synthesis or reconstruction of a signal in the wavelet packet scheme is a similar process to the wavelet reconstruction presented before. We start at leave nodes and from one approximation and one detail node we reconstruct its father with filters H and G , and in this way and recursively until we arrive to the initial image. In the example of Fig. 2.6 and starting from the bold-faced nodes we perform the next steps: a) from sds and dds we get ds_0, ds_1 , b) from ss and ds coefficients we get s coefficients, c) finally, from s and d we get the initial signal x . Several implementations of the analysis and synthesis with wavelet packets can be found in [106].

There are some techniques oriented to find the best basis for a signal without calculating all the tree [105]. To choose a base means to select those nodes that permits reconstruction. These techniques achieve the best basis in relation to some criterion as minimal entropy of the coefficients. Wavelet packets analyze both branches in the same way and this permits to adapt better to the frequency content of the signal. The election of the wavelet function in the analysis should be done taking into account the data. And the election of the base used in the synthesis must be designed taking into account the specific problem: compression, classification, recognition, etc.

2.2.7 Extension to 2D

Gabor filters

To extent Gabor filters to two dimensions we take the underlying idea of the 1D Gabor filters, to modulate a complex exponential with a Gaussian, with and increase of the number of parameters.

- There are two modulation frequencies (u_0, v_0) . The direction of modulation is $\theta_0 = \tan^{-1}(v_0/u_0)$, in which the spatial frequency is $\omega_0 = \sqrt{u_0^2 + v_0^2}$.
- The Gaussian window is bidimensional, therefore we can have different variances for each axis, σ_u, σ_v . The expressions of this 2D Gabor filter at spatial and frequency domains are:

$$g(x, y) = e^{-\frac{1}{2}[\frac{x^2}{\sigma_x^2} + \frac{y^2}{\sigma_y^2}]} e^{j2\pi(u_0 x + v_0 y)} , \quad (2.40)$$

$$G(u, v) = A e^{-\frac{1}{2}[\frac{(u-u_0)^2}{\sigma_u^2} + \frac{(v-v_0)^2}{\sigma_v^2}]} , \quad (2.41)$$

with $A = 2\pi\sigma_x\sigma_y$, $\sigma_u = 1/2\pi\sigma_x$, $\sigma_v = 1/2\pi\sigma_y$.

- When $\sigma_u \neq \sigma_v$, Gaussian function is not isotropic. For non-isotropic functions we can also add a new parameter in order to take into account an angle of rotation. This angle has not been included in Eq. (2.40) and (2.41).

The 2D Gabor transform is a complex 4D function $G(x_0, y_0; u_0, v_0)$ similar to the STFT, that describes in each point (x_0, y_0) the spectral contents of an image $f(x, y)$. Gabor filters are well localized in spatial and frequency domains and achieve the minimum uncertainty. Nevertheless, equations (2.40), (2.41) are not used to process images. It is possible to rewrite them to obtain a family of functions with the next features:

- All the functions can be expressed as a dilation, translation and rotation of a mother Gabor function, as wavelets do, for this reason we call them Gabor wavelets.
- Previous property of well localization is preserved.

Let us define two new parameters: orientation bandwidth, B_θ , and frequency bandwidth, B_ω , which fix the number of possible orientations, N , and the number of frequency bands for each orientation, M (see Fig. 2.7). A more easy and compact way to describe a Gabor filter bank is from M, N parameters and its expression in polar form:

$$g_{m,n}(\omega, \theta) = e^{-(\omega-\omega_{0,m})^2/2\sigma_{\omega,m}^2} e^{-(\theta-\theta_{0,n})^2/2\sigma_{\theta,n}^2} , \quad (2.42)$$

with $1 \leq m \leq M, 1 \leq n \leq N$. The angular and radial variances are:

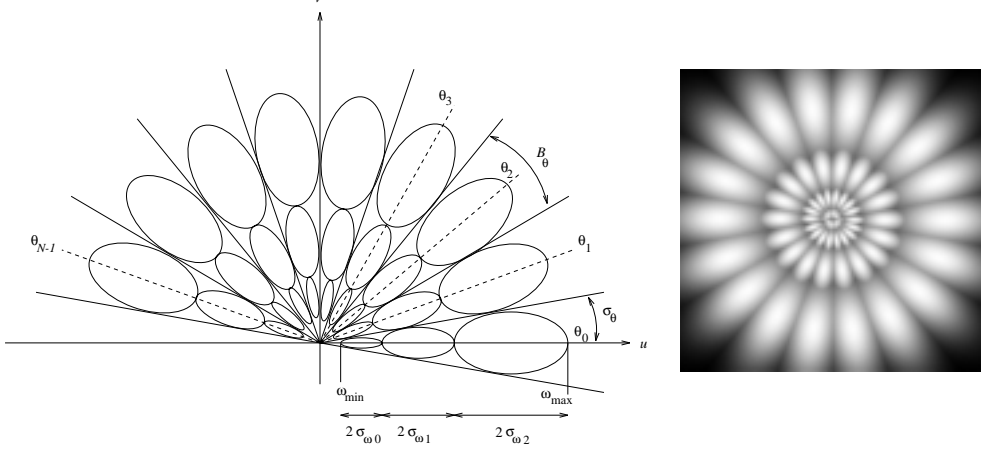


Figure 2.7: Parameters of the Gabor filters and bank of filters for $M = 4$ bands and $N = 9$ orientations

$$\sigma_\theta = \frac{1}{2}B_\theta = \frac{1}{2} \frac{\pi}{N}, \quad (2.43)$$

$$\sigma_{\omega,0} = (\omega_{\max} - \omega_{\min}) / (2(2^M - 1)), \quad (2.44)$$

$$\sigma_{\omega,m} = 2^{B_\omega(m-1)} \sigma_{\omega,0}, \quad (2.45)$$

$\omega_{\min}, \omega_{\max}$ are the limit frequencies where we want to place the Gabor filters, that is, $\omega_{\min} \leq \sqrt{u^2 + v^2} \leq \omega_{\max}$. Frequently, $\omega_{\min} > 0$ in order to do not use the continuous component of the image. $\sigma_{\omega,0}$ is the radial width of the first band and $\sigma_{\omega,m}$ of the m -th band. Often, $B_\omega = 1$ is chosen equal to one octave. In this case, the centers in polar coordinates are:

$$\theta_{0,n} = 2\sigma_\theta(n-1), \quad (2.46)$$

$$\omega_{0,m} = \omega_{\min} + \sigma_{\omega,0}[1 + 3(2^{(m-1)} - 1)], \quad (2.47)$$

again for $1 \leq m \leq M, 1 \leq n \leq N$.

Wavelets and wavelet packets

If we want to extend the orthogonal scheme presented in Sec. 2.2.4 to the two-dimensional case we can follow two direction [90]. See Fig. 2.8 to identify any of these two approaches.

In the first one, known as the standard decomposition, we apply the one-dimensional transform to each of the axes. This is done in a similar way as FFT extends to 2D. First, all the rows are transformed with the 1D transform with all the levels we want to expand. Then, we treat these transformed rows as if they were themselves an

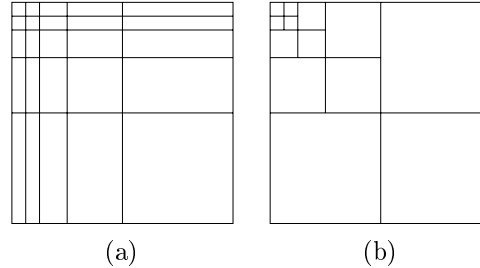


Figure 2.8: (a) Standard 2D wavelet decomposition, (b) nonstandard decomposition (MRA).

image and apply the same transform to each column. The final 2D transformation can be expressed as a decomposition over a base of 2D orthogonal wavelets. The elements of this base are all the possible tensor products of the elements of the 1D base ($\psi_i(x)\psi_j(y)$). The major drawback of this transformation is that the aspect ratio of the details is not preserved due to the non-square support of some elements of the wavelet base.

The second way of extending from one-dimensional to two-dimensional transformation is known as the nonstandard decomposition. It is the solution adopted by the image processing community. It preserves the aspect of the image at each scale. The MRA proposed by Mallat [62] use this technique to achieve the result and alternates the 1D wavelet transformation of rows and columns at each level of the decomposition. Here, we have expressed the initial signal as a decomposition in a wavelet base but unlike previous case, elements of this base at each level i one of these wavelets: $\phi_i(x)\psi_i(y)$, $\psi_i(x)\phi_i(y)$, $\psi_i(x)\psi_i(y)$. This is the most used scheme for bidimensional decompositions of images, it keeps the size of any detail proportional to the initial image, and computation of the nonstandard is slightly more efficient.

Concerning to wavelet packets, we see in Sec. 2.2.6 that it works as a MRA where at each moment in the decomposition we can choose to decompose approximation or details, in the two-dimensional case these details can be any of the tree pinpointed before. The extension to 2D needs of the nonstandard decomposition as in the MRA.

***À trous* algorithm**

As in the previous case, *à trous* algorithm can be extended to 2D if we use separable filters in the decomposition. At each level we must to perform the convolution of the image with a filter in the x axis and then, the convolution in the other axis. The filters we use in our work are a family of functions named the B-splines. This family of filters can be built easily from the convolution of a basic box function (B_0) with itself; after, we have the triangle function (B_1), etc. Higher is the index of the spline function more similar is to a Gaussian.

As we see in Sec. 2.2.5, this algorithm is translation-invariant that is a good property. Using the B-spline family we achieve a new good property, symmetry of the functions used in the analysis that is not possible in the basic MRA scheme. And, if

we use high index in this family we come closer to an isotropic functions also useful for analysis.

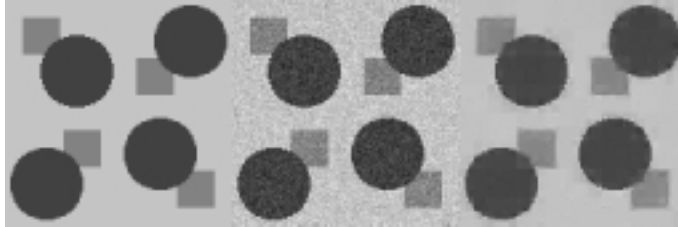


Figure 2.9: Filtered images with soft thresholding.

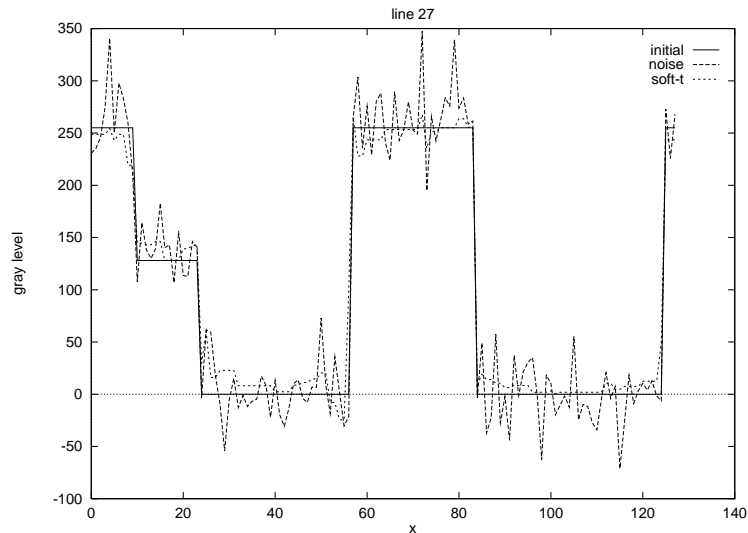


Figure 2.10: Profiles of: initial image, image with noise added and filtered image.

2.2.8 Applications

The usefulness of wavelets as a tool to solve a lot of problems inside the computer vision field is supported by the big amount of works published in this area. As a little summary of these possibilities we go to emphasized some aspects that were the starting point in our work. We start in this field implementing some wavelet decomposition algorithm and performing with them a few and basic applications. In this section we go to fast review some of these applications.

Summarizing most of the next approaches we see that wavelets have the interesting property of group important information in order to describe the image in a few and differentiate coefficients. Selecting and filtering these coefficients we can achieve the different solutions. The presentation we do in this part is also as an introduction in

order to shows the power and versatility of these tools in the image processing field. These applications have also and important theoretical background that has been relaxed for the sake of the explanation.

Filtering

Working with images involves sometime doing assumptions that come from other fields in order to apply specific algorithms. It is the case of linear filtering that supposes images as stationary process. Really, most images are not stationary and discontinuities are those zones in which the information is. Wavelets are well adapted to the study of discontinuities and therefore filtering using these non-linear schemes achieves better results than linear ones.

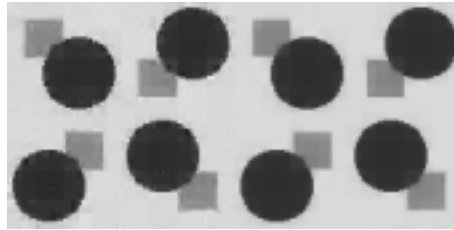


Figure 2.11: Filtered image and average of 9 translated and filtered images.

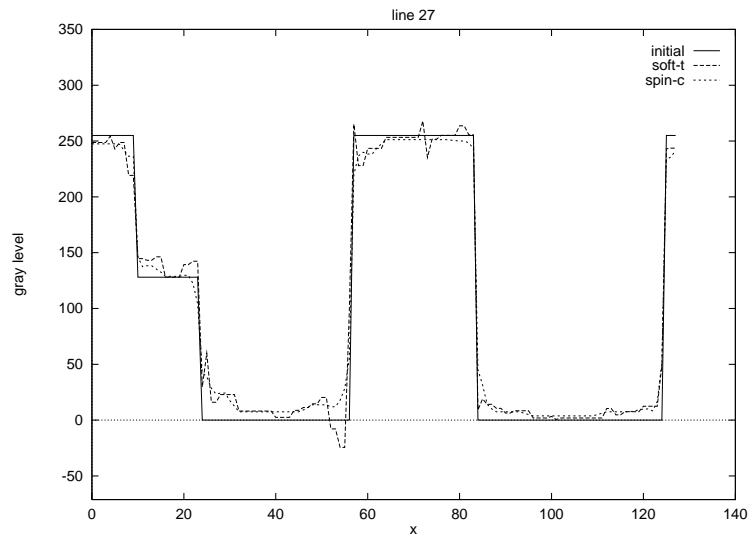


Figure 2.12: Profiles of: initial image, filtered image and averaged and filtered images.

Donoho's work [26] propose a non-linear approach to filter a signal. The principal idea is that important information of non-stationary signals is concentrate in discontinuities that gives the highest coefficients in a wavelet decomposition. However, noise

gives rise to a nearly constant level of small coefficients. Filter process is performed choosing a threshold level t in the coefficients of the decomposition and putting to zero all those with its absolute value is lower than the threshold (see Eq. (2.48)). This value is related to the power of noise in the image as Eq. (2.49) shows. This technique is named *soft thresholding* [25] and example of its application can be showed in Figs. 2.9 and 2.10. Some drawbacks of this techniques as the non-translation invariance can be solved applying other approaches as the *spinning cycle* procedure [18] that implies to average the results of the same process applied to translations of the signal (see Figs. 2.11 and 2.12).

$$st_u(x) = \begin{cases} \text{sign}(x)(|x| - u) & \text{if } |x| > u \\ 0 & \text{if } |x| \leq u \end{cases} . \quad (2.48)$$

$$t = \sqrt{2 \log(n)} \sigma / \sqrt{n} . \quad (2.49)$$

Compression

Compression is a field where wavelets have beaten other decomposition schemes. As an interesting case we can analyze the compression of static images as JPEG where previous version was based on the discrete cosine transform well suited for stationary signals that gave good results over images. Now, the new standard [43], named JPEG 2000, is intended to provide a new image coding system using state of the art compression techniques. It changes previous decomposition schemes based on DCT introducing the use of wavelet technology. Results we obtain with this new scheme are visually better than before and also reducing some drawbacks of the previous scheme as blocking. See reference [82] in order to compare this new standard with some common compression algorithms.

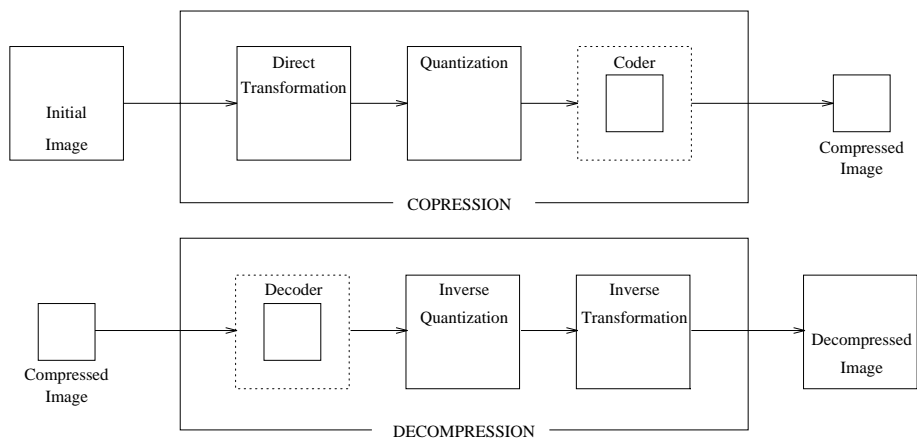


Figure 2.13: Compression and reconstruction scheme.

Instead of analyze this standard we go to emphasize the principal idea of the compression schemes based on wavelets. In we visualize a wavelet decomposition

we see that most of the coefficients are zero or closer to zero. As we say before, important information is represented in few coefficients with high values. Compression is achieved choosing a new threshold t saving only high values and it is done collapsing coefficients to zero (see Eq. (2.50)). Sometimes, compression schemes take profit of the redundancy of coefficients over scales; then we need to analyze and save the decomposition tree [87, 80]. Previous considerations are those related to the early decomposition stages, but to achieve the final result some other step must be done as quantization and coding of the data. The entire process of compression decompression is showed in the scheme of Fig. 2.13.

$$ht_u(x) = \begin{cases} x & \text{if } |x| > u \\ 0 & \text{if } |x| \leq u \end{cases} . \quad (2.50)$$

We go to present some compression results based on the hard-thresholding of coefficients (Eq. (2.50)) over a fingerprint image as an example of the possibilities of this method and to show how results are degraded. We use MRA decomposition with different thresholds and different decomposition basis. Results are summarized in Fig. 2.14.










Filter	u = 10	u = 50	u = 100
dau2	 45%	 7%	 2%
dau8	 27%	 6%	 2%
dau16	 24%	 6%	 2%

Figure 2.14: Compression of a fingerprint image using hard-thresholding.

The compression rates represent the percentage of coefficient greater than a threshold; therefore they can be reduced with the quantization and a codification steps.

Data fusion

Finally, an interesting application that we will use in Sec. 4.5.2 is related to data fusion. Here, we have different source of information that comes from the same origin and as result we want to summarize it choosing the more important of each one. Again, wavelets are well adapted to perform this task of emphasizing which is the relevant information and where is it. Then, choosing among the most important coefficients (higher absolute values) of each source and reconstructing we obtain the expected result [47].

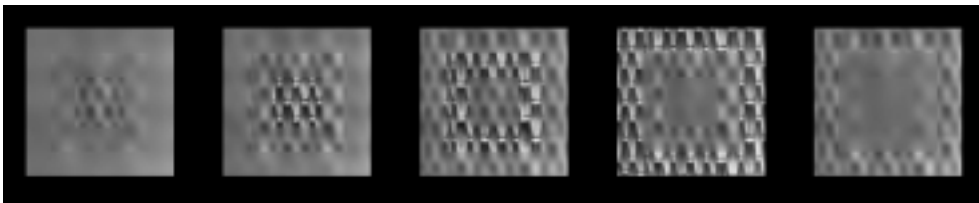


Figure 2.15: Pyramid.

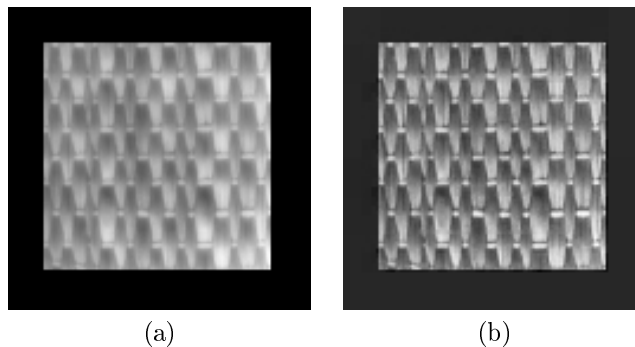


Figure 2.16: (a) Averaged images, (b) focused by means of the wavelet transform.

We use that in order to focus microscopic images. If we see a sample through the microscope at high magnification we realize that it is not focused entirely and we need to move up and down to visualize it correctly. Wavelets applied over these images gives high coefficient in those focused zones. Taking several images at different depth we can select the highest coefficients on each image. Reconstruction from this selection of coefficients gives us the focused image and also we can compute the depth map of the sample. Figures 2.15 and 2.17 show a set of images partly out of focus, the first one is a synthetic sequence and the second one a real case. Figures 2.15 and 2.17 show results from the previous sequences with the proposed algorithm and an averaged solution for comparison purposes.

The technique we have explained can be extended easily to other kind of images as multichannel images from remote sensing, or medical images.

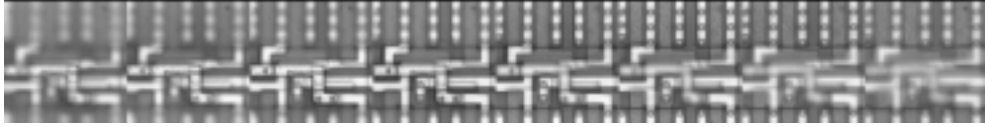


Figure 2.17: Circuit.

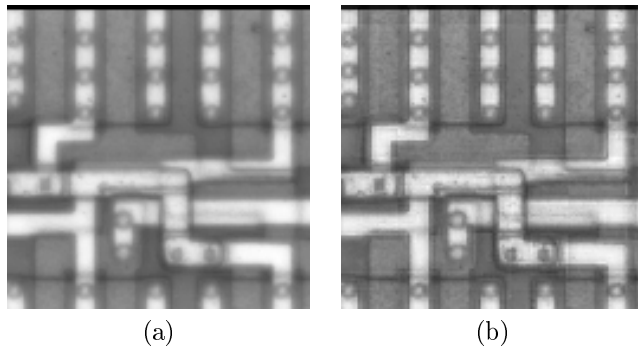


Figure 2.18: (a) Averaged images, (b) focused by means of the wavelet transform.